

Targeted delivery of methotrexate to epidermal growth factor receptor–positive brain tumors by means of cetuximab (IMC-C225) dendrimer bioconjugates

Gong Wu,¹ Rolf F. Barth,¹ Weilian Yang,¹ Shinji Kawabata,¹ Liwen Zhang,² and Kari Green-Church²

¹Department of Pathology and ²Mass Spectrometry and Proteomics Facility, The Ohio State University, Columbus, Ohio

Abstract

We have constructed a drug delivery vehicle that targets the epidermal growth factor receptor (EGFR) and its mutant isoform EGFRvIII. The monoclonal antibody, cetuximab, previously known as C225, which binds to both EGFR and EGFRvIII, was covalently linked via its Fc region to a fifth-generation (G5) polyamidoamine dendrimer containing the cytotoxic drug methotrexate. As measured by mass spectrometry and UV/vis spectroscopy, the resulting bioconjugate, designated C225-G5-MTX, contained 12.6 molecules of methotrexate per unit of dendrimer. Specific binding and cytotoxicity of the bioconjugate was evaluated against the EGFR-expressing rat glioma cell line F98_{EGFR}. Using a competitive binding assay, it was shown that the bioconjugate retained its affinity for F98_{EGFR} cells, with a 0.8 log unit reduction in its EC₅₀. Only cetuximab completely inhibited binding of the bioconjugate, which was unaffected by methotrexate or dendrimer. Cetuximab alone was not cytotoxic to F98_{EGFR} cells at the concentration tested, whereas the IC₅₀ of the bioconjugate was 220 nmol/L, which was a 2.7 log unit decrease in toxicity over that of free methotrexate. The biodistribution of C225-G5-MTX in rats bearing i.c. implants of either F98_{EGFR} or F98_{WT} gliomas was determined 24 hours following convection enhanced delivery of ¹²⁵I-labeled bioconjugate. At this time, 62.9 ± 14.7% ID/g tumor was localized in rats bearing F98_{EGFR} gliomas versus 11.3 ± 3.6% ID/g tumor in animals bearing F98_{WT} gliomas, thereby showing specific molecular targeting of the tumor. The corresponding radioactivity of normal brain from the F98_{EGFR} tumor-bearing right

and non-tumor-bearing left cerebral hemisphere were 5.8 ± 3.4% and 0.8 ± 0.6% ID/g, respectively. Based on these results, therapy studies were initiated in F98_{EGFR} glioma-bearing rats. Animals that received C225-G5-MTX, cetuximab, or free methotrexate had median survival times of 15, 17, and 19.5 days, respectively, which were not statistically different from each other or untreated control animals. Our results, which are both positive and negative, show that specific molecular targeting is but one of several requirements that must be fulfilled if an antibody-drug bioconjugate will be therapeutically useful. [Mol Cancer Ther 2006;5(1):52–9]

Introduction

Targeted drug delivery by means of monoclonal antibodies (mAb) has attracted substantial attention for cancer therapy (1–4). Using tumor-specific antigens or antibodies as targeting moieties, cytotoxic drugs can be selectively delivered to tumor cells, thereby reducing the drug concentration in normal tissues and its toxic side effects (5, 6). Malignant gliomas are among the most therapeutically refractory of all cancers (7, 8), and there is a continuing need to develop more effective strategies for their treatment. The epidermal growth factor receptor (EGFR) and its mutant isoform, EGFRvIII, frequently are overexpressed in malignant gliomas (9–11). EGFR is a transmembrane receptor containing an extracellular ligand-binding domain, a transmembrane domain, and an intracellular tyrosine kinase domain (9). Ligand binding results in homodimerization and heterodimerization with various family members. This facilitates autophosphorylation of tyrosine residues in the carboxyl terminus of the dimer, which can then regulate downstream signaling pathways, including cell division, adhesion, motility and invasiveness, resistance to apoptosis, intracellular vesicle trafficking, and angiogenesis (12). EGFRvIII results from a nonrandom 801-bp in-frame deletion of exons 2 to 7 of the EGFR gene. It can be activated independent of ligand binding, is not expressed in normal tissues, and has been regarded as a tumor-specific marker (13–15).

Due to the important role of EGFR and EGFRvIII in the development of malignant gliomas, a variety of agents targeting either the extracellular ligand-binding domain or the intracellular tyrosine kinase region of EGFR are currently among the most promising therapeutics under clinical evaluation (16, 17). These EGFR inhibitors can induce cell apoptosis, suppress cell migration, disrupt angiogenesis, reverse resistance to cytotoxic drugs, and cause tumor regression. Cetuximab (Erbix or IMC-C225), which is directed against both wild-type EGFR and EGFRvIII, has been one of the most intensively studied

Received 8/17/05; revised 9/29/05; accepted 11/2/05.

Grant support: NIH grant 1R01CA098945-02.

The costs of publication of this article were defrayed in part by the payment of page charges. This article must therefore be hereby marked advertisement in accordance with 18 U.S.C. Section 1734 solely to indicate this fact.

Requests for reprints: Rolf F. Barth, Department of Pathology, The Ohio State University, 165 Hamilton Hall, 1645 Neil Avenue, Columbus, OH 43210. Phone: 614-292-2177; Fax: 614-292-7072. E-mail: barth.1@osu.edu

Copyright © 2006 American Association for Cancer Research.

doi:10.1158/1535-7163.MCT-05-0325

mAbs directed against the receptor (18, 19). It has been approved for use in combination with either 5-fluorouracil or irinotecan for the treatment of patients with EGFR-expressing metastatic colorectal cancer (20, 21). Because cetuximab and most cytotoxic drugs have different modes of action, the combination of these two agents, either independently or as a bioconjugate, is an attractive drug-targeting strategy for cancer treatment. There are two possible ways to assemble such complexes. (a) Cetuximab can be linked directly to the drug. An example of this was the linkage of paclitaxel (Taxol) to cetuximab by Safavy et al. (22), who have reported enhanced *in vitro* cytotoxic activity compared with that of free drug, intact antibody, or a mixture of the two. However, in studies in nude mice bearing A431 human squamous cell carcinoma, the bioconjugate and C225 had similar *in vivo* activity. This may have been due to either a relatively low dose of the drug delivered by the antibody or its suboptimal release. (b) Cetuximab could be linked to liposomes. Liposome-encapsulated doxorubicin, vinorelbine, and methotrexate have been prepared to improve its drug-loading capacity (23). In each case, the immunoliposomes were significantly more cytotoxic to the target cells than the corresponding nontargeted liposomal drug. These results showed that EGFR-targeted immunoliposomes could efficiently deliver anticancer drugs to receptor-overexpressing cells. However, due to their large size, drugs encapsulated in immunoliposomes have their own limitations. If given systemically, only very small quantities reach the brain tumor due to the blood-brain barrier. However, direct intracerebral (i.c.) administration of liposomes by convection enhanced delivery (CED) to glioma-bearing rats resulted in extensive distribution to the tumor and extension into surrounding normal brain (23).

To enhance drug delivery, we have used a polyamidoamine dendrimer as a drug carrier for methotrexate. Methotrexate is a folate antimetabolite and a potent anticancer agent of proven efficacy for the treatment of a variety of malignant tumors (24). Polyamidoamine (PAMAM) dendrimers potentially are ideal drug carriers because of their well-defined structure and high density of functional groups. The purpose of the present study was to determine if a cetuximab-dendrimer-methotrexate bioconjugate had the requisite properties for treatment of an experimental rat glioma. In this report, we describe the preparation and *in vitro* and *in vivo* evaluation of a bioconjugate produced by site-specific linkage of cetuximab to a fifth-generation (G5) PAMAM dendrimer coupled to methotrexate.

Materials and Methods

Synthetic and Analytic Materials and Supplies

Methotrexate and a fifth-generation PAMAM dendrimer, containing 128 reactive terminal amine groups, were purchased from Sigma-Aldrich Corp. (St. Louis, MO). *N*-succinimidyl-3-(2-pyridyldithio)propionate (SPDP) and *N*-(κ -maleimidoundecanoic acid) hydrazide were obtained from Pierce (Rockford, IL). Other chemicals were of reagent grade and were purchased from several chemical

supply companies. Cetuximab was generously provided by Dr. Daniel Hicklin (Vice President for Research, ImClone Systems, Inc., New York, NY). Stirred cell/ultrafiltration membranes (MWCO 100,000) were purchased from Fisher Scientific (Pittsburgh, PA). PD-10 disposable columns, Sephadex G25, and Sephacryl S-300 were purchased from Amersham Pharmacia Biotech (Piscataway, NJ). UV measurements were determined by means of a Beckman DU6 recording spectrophotometer (Beckman, Fullerton, CA). The protein concentrations of cetuximab and the bioconjugate were determined by UV absorption spectrometry at 280 and 595 nm, respectively, using a Coomassie blue protein assay reagent (Pierce). All measurements were made against known concentrations of cetuximab as a reference standard. The concentrations of SPDP in the SPDP-G5 conjugate were determined by UV spectrometry at 343 nm following cleavage of the disulfide bond by DTT. Methotrexate was quantified by its absorbance at 372 nm.

Preparation of the Bioconjugates

Linkage of methotrexate and SPDP-G5 was carried out with 1-ethyl-3(3-dimethylaminopropyl)carbodiimide hydrochloride and *N*-hydroxysuccinimide (Fig. 1). Briefly, 10 mg methotrexate (22 μ mol/L) was dissolved in 50 mmol/L phosphate buffer (pH 6.0) containing 21 mg 1-ethyl-3(3-dimethylaminopropyl)carbodiimide hydrochloride (0.11 mmol/L) and 19 mg *N*-hydroxysuccinimide (0.16 mmol/L). The mixture was stirred for 15 minutes at ambient temperature and added to 4.81 mg SPDP-G5 (0.17 μ mol/L) solution (pH 8). The reaction mixture was stirred for another 4 hours at ambient temperature. The procedure for linking modified dendrimer to cetuximab has been described previously (25). To test the stability of the bioconjugate, 0.5 mL C225-G5-MTX in PBS was incubated at 37°C. An aliquot of sample was removed at different time points and desalted and the methotrexate content was measured by UV/vis spectroscopy at 372 nm.

Characterization of the Bioconjugate by Mass Spectrometry

Matrix-assisted laser desorption/ionization time-of-flight mass spectrometry was carried out at the Mass Spectrometry and Proteomics Facility at the Ohio State University (Columbus, OH). To prepare a sample for mass spectrometry analysis, the G5-MTX conjugate was desalted on a PD-10 column and eluted with water. A stock solution of the dendrimer or G5-MTX was prepared by dissolving it in 50% methanol. Matrix-assisted laser desorption/ionization time-of-flight mass spectrometry was done on a Reflex III (Bruker Daltonics, Inc., Billerica, MA) mass spectrometer

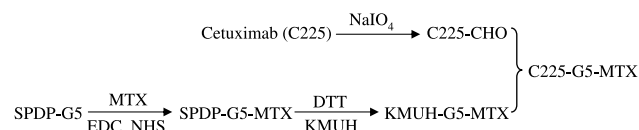


Figure 1. Schematic representation of the linkage of methotrexate-containing dendrimer to cetuximab. *MTX*, methotrexate; *EDC*, 1-ethyl-3(3-dimethylaminopropyl)carbodiimide hydrochloride; *NHS*, *N*-hydroxysuccinimide; *KMUH*, *N*-(κ -maleimidoundecanoic acid) hydrazide.

operated in the linear, positive ion mode at an accelerating voltage of 28 kV. The N₂ laser was operated at the minimum threshold level required to generate a signal and minimize dissociation. The instrument was calibrated and the matrix, sinapinic acid, was prepared as a saturated solution in 50% acetonitrile with 0.1% trifluoroacetic acid in water. Aliquots consisting of 5.0 μL matrix and 1.0 μL sample were thoroughly mixed, spotted on the target plate (1.0 μL), and allowed to dry before analysis.

Radiolabeling of Bioconjugate

Radiolabeling of C225-G5-MTX with either ¹³¹I or ¹²⁵I was carried out using Iodo-Gen precoated iodination tubes according to the procedure described by the manufacturer (Pierce). Briefly, 10 μL (1.0 mCi) carrier-free Na¹³¹I or Na¹²⁵I (ICN Biomedicals, Inc., Costa Mesa, CA) and 50 μL of 100 mmol/L phosphate buffer (pH 7.5; 0.1 mol/L NaCl) were added to the precoated tubes. After incubating them for 6 minutes at ambient temperature, the activated iodide was removed and added to the antibody solution (50 μg/50 μL) and then incubated for an additional 9 minutes. Radiolabeled bioconjugate was purified on a Bio-Spin 30 Tris column (Bio-Rad Laboratories, Hercules, CA) by elution with 25 mmol/L phosphate buffer (pH 7.5). Protein-bound and free ¹³¹I or ¹²⁵I were determined by precipitation with TCA and γ-scintillation counting using a well counter (TM Analytic, Des Plaines, IL).

Cell Culture

The F98 glioma cell line (ATCC CRL-2397) was derived from a glioma that developed in the progeny of pregnant Fischer rats following the administration of *N*-ethyl-*N*-nitrosourea (26). This cell line has been used extensively by us for studies relating to BNCT (25–29). EGFR-expressing F98 glioma cells (F98_{EGFR}) were produced by transfecting wild-type cells (F98_{WT}) with an expression vector containing human EGFR cDNA as described recently in detail elsewhere (30). F98_{EGFR} cells were maintained and propagated in DMEM containing 100 units/mL penicillin, 100 μm/mL streptomycin, 200 μg/mL G418, and 10% fetal bovine serum (Life Technologies, Inc., Rockville, MD). F98_{WT} cells were cultured in the same medium lacking G418 at 37°C in a humidified atmosphere containing 5% CO₂.

Competitive Binding Assay

F98_{EGFR} cells were seeded into T-150 flasks and cultured for 2 days to establish confluent monolayers, following which they were washed twice with PBS and then disaggregated by incubating them with 0.5 mmol/L EDTA at 37°C for 10 minutes. Following removal of EDTA, 10⁶ cells were added to 1.5 mL tubes to which 2.0 nmol/L [¹²⁵I]cetuximab and varying amounts of either unmodified cetuximab or C225-G5-MTX in 0.1% bovine serum albumin had been added, and these were incubated at 4°C for 90 minutes. The cells then were washed thrice with PBS and the cell-bound [¹²⁵I]cetuximab was separated from free [¹²⁵I]cetuximab by centrifugation, following which radioactivity was determined by γ-scintillation counting. To determine the binding contribution of each component of the bioconjugate, 2 nmol/L [¹²⁵I]C225-G5-MTX was added to each vial containing 10⁶ F98_{EGFR} cells. Then, either

35 μmol/L methotrexate, 2.0 μmol/L cetuximab, 2.0 μmol/L G5, or a mixture of 35 μmol/L methotrexate and 2.0 μmol/L cetuximab were added. After incubation at 4°C for 90 minutes, the cells were washed thrice with PBS and cell-bound radioactivity was determined by γ-scintillation counting.

Cytotoxicity Assay

Specific cytotoxicity of the EGFR-targeted, methotrexate-containing bioconjugate was evaluated using tumor cells plated at a density of 5,000 per well in 96-well Costar plates (Corning, Inc., Corning, NY) and then allowed to grow overnight. Fresh medium containing varying amounts of C225-G5-MTX, methotrexate, or cetuximab, was added and incubated for another 72 hours at 37°C. Cells were fixed by slowly adding 50 μL cold 50% TCA to each well and then held at 4°C for 1 hour. Cell viability was analyzed by using the sulforhodamine B cell proliferation assay (31) and absorbency was measured at 490 nm in a 96-well microplate reader (Dyex Technologies, Inc., Chantilly, VA).

Tumor Model and Biodistribution of [¹²⁵I]C225-G5-MTX

Fischer rats were purchased from the Animal Production Branch, National Cancer Institute, Frederick Research Laboratory (Frederick, MD). Procedures to minimize discomfort, pain, and distress were in accordance with the USPHS Policy on Humane Care and Use of Laboratory Animals. When implanted i.c. into syngeneic Fischer rats, the F98_{WT} and F98_{EGFR} cell lines grow as a discrete mass with a peripheral zone of infiltrating tumor cells. These tumor models have been used for a variety of experimental brain tumor studies. F98_{WT} or F98_{EGFR} cells (10⁵) were stereotactically implanted into the right caudate nucleus of Fischer rats as described previously (30). Biodistribution studies were initiated 12 to 14 days following CED of 5 μCi [¹³¹I]C225-G5-MTX (0.63 μg) via the central entry port of a plastic screw, which has been embedded into the calvarium at the time of tumor implantation. CED was carried out as described in detail elsewhere (32). The test agent (10 μL) was given over 30 minutes using a 20 μL Hamilton syringe fitted with a 27-gauge needle. Rats were euthanized 24 hours later; tumor, normal brain, blood, liver, kidneys, and skin radioiodine samples were taken; and biodistribution was determined by γ-scintillation counting for radioiodine. Five animals were used per group and the %ID/g was calculated.

Therapy Experiments

Therapy studies were carried out 7 days following stereotactic implantation of 10⁵ F98_{EGFR} glioma cells. Initially, to establish a safe dose of the bioconjugate, two rats received 40 μg methotrexate and another two animals received 400 μg methotrexate by means of CED, and both doses were well tolerated. Therefore, for therapy studies, rats received 10 μL methotrexate (3.5 μg/μL), C225-G5-MTX (3.5 μg/μL methotrexate), or cetuximab alone by means of CED given over 30 minutes. Animals were divided into three groups of 6 to 10 rats each. Clinical status of the animals was monitored and rats were weighed thrice weekly. Premoribund animals, as defined by a 30% loss in

weight over 3 days with a concomitant reduction in physical activity, were euthanized. Their brains were removed, fixed in formalin, and then cut coronally at the level of the optic chiasm and 2 mm anterior and posterior to it. Sections were embedded in paraffin, cut at 4 μm , stained with H&E, and then examined microscopically to assess histopathologic changes and the tumor size. The mean and median survival times in days after tumor implantation were calculated and Kaplan-Meier survival curves were plotted. The percent increased life span was determined as described previously (28). Gehan's Wilcoxon rank sum test was applied to determine the levels of significance in survival times between different groups of treated animals (33).

Results

Characterization of the Bioconjugate

As shown in Fig. 1, the linkage of methotrexate to polyamidoamine dendrimers was carried out by the carbodiimide reaction in which one carboxyl group of methotrexate was linked to the primary amine group of the dendrimer to form a covalent α -amide bond. There was no precipitation when methotrexate and the primary amine groups were reacted at a 1:1 ratio. Ratios of 1:1.5 and 1:2 also were tested, but with both of these significant amounts of a yellow, water-insoluble precipitate formed. The number of methotrexate molecules attached to each unit of dendrimer was determined by matrix-assisted laser desorption/ionization time-of-flight mass spectrometry. As shown in Fig. 2A, there were three peaks at m/z : 13,820, 26,574, and 51,425. The major peak was at m/z 26,574, which corresponded to 92.2% of monodendrimer, based on a theoretical molecular weight of 28,826 Da for G5. The two other small peaks represented the fourth-generation dendrimer (or 2+ ion of G5) and sixth-generation dendrimer, respec-

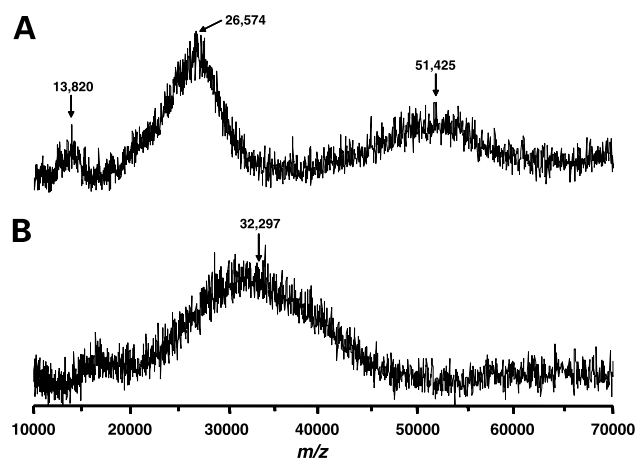


Figure 2. Matrix-assisted laser desorption/ionization time-of-flight mass spectrometry of fifth-generation polyamidoamine dendrimer G5 (A) and MTX-G5 (B). The matrix was composed of a saturated sinapinic acid in 50% acetonitrile and 1% trifluoroacetic acid. Aliquots of matrix and sample (5:1 ratio) were spotted on the plate and data were collected on a Reflex III mass spectrometer in positive ion mode.

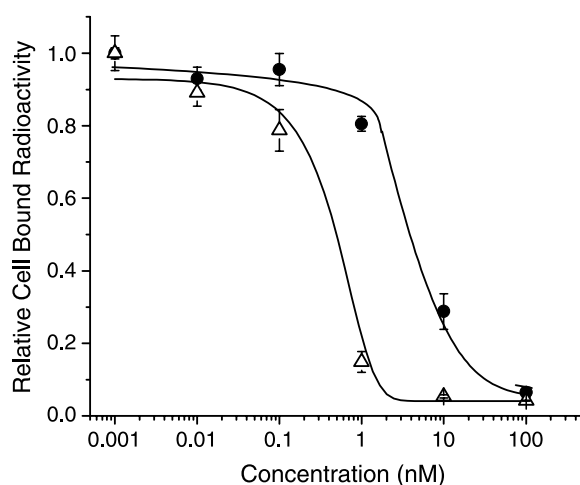


Figure 3. Competitive binding assay. F98_{EGFR} cells were incubated with [¹²⁵I]cetuximab and varying amounts of nonradiolabeled cetuximab (Δ) or C225-G5-MTX (●) at 4°C for 90 min. Cell-bound radioactivity was determined by γ -scintillation counting.

tively. The molecular weight after linkage of methotrexate to G5 is shown in Fig. 2B. The average molecular weight of the large broad peak was 32,297 Da. This was an increase of 5,723 Da, which indicated that the number of methotrexate molecules per molecule of G5 was 12.6. The linkage of the methotrexate-dendrimer complex to cetuximab was carried out by means of two heterobifunctional linkers, SPDP and *N*-(κ -maleimidoundecanoic acid) hydrazide, as described previously (25). The final bioconjugate was purified by Sephacryl S-300 chromatography, and based on the concentration of protein and methotrexate, approximately one dendrimer was linked to each molecule of cetuximab. As determined by UV/vis spectrometry, the bioconjugate was stable for at least 14 days.

Competitive Binding and Cytotoxicity Assays

The competitive binding of C225-G5-MTX with radiolabeled cetuximab (Fig. 3) showed that the bioconjugate retained its ability to bind to EGFR. The EC₅₀ of cetuximab and C225-G5-MTX were 0.49 and 3.4 nmol/L, respectively. As shown in Fig. 4, only cetuximab competed with the bioconjugate to bind to EGFR. In the presence of 2.0 $\mu\text{mol/L}$ cetuximab or a combination of 2.0 $\mu\text{mol/L}$ cetuximab and 35 $\mu\text{mol/L}$ methotrexate, the binding of [¹²⁵I]C225-G5-MTX to F98_{EGFR} cells decreased to $16.6 \pm 2.8\%$ and $21.6 \pm 0.3\%$, respectively. The addition of 35 $\mu\text{mol/L}$ methotrexate had little or no inhibitory effect on the binding of the bioconjugate, which retained $97.3 \pm 1.6\%$ of its binding affinity compared with the control. However, the addition of 2.0 $\mu\text{mol/L}$ G5 resulted in an increase to $121.6 \pm 0.9\%$ compared with the control. This was attributed to the fact that the dendrimer, which also has been used as a nonviral transfecting agent, bound to the cell membrane via electrostatic interactions and induced membrane bending, thereby facilitating endocytosis of the bioconjugate. As shown in Fig. 5, cetuximab was not cytotoxic to F98_{EGFR} cells at the concentrations tested, whereas free methotrexate was highly

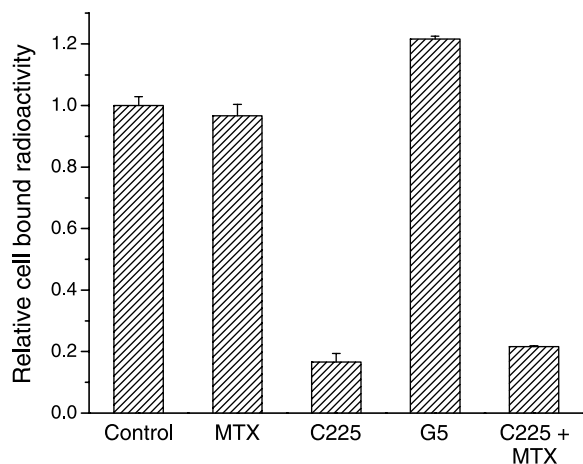


Figure 4. Competitive binding assay with components of bioconjugate. [^{125}I]C225-G5-MTX (2 nmol/L) was added to vials contains 10^6 F98_{EGFR} cells. Then, either 35 $\mu\text{mol/L}$ methotrexate, 2.0 $\mu\text{mol/L}$ cetuximab, 2.0 $\mu\text{mol/L}$ G5, or a physical mixture of 35 $\mu\text{mol/L}$ methotrexate and 2.0 $\mu\text{mol/L}$ cetuximab were added. After incubating at 4°C for 90 min, the cell-bound radioactivity was measured by γ -scintillation counting. Only C225 inhibited binding of the bioconjugate.

cytotoxic to F98_{EGFR} cells with an IC_{50} of 0.42 nmol/L. After linking cetuximab to the methotrexate-dendrimer complex, the bioconjugate had an IC_{50} of 220 nmol/L, which was 2.7 units less toxic than free methotrexate.

Biodistribution following Intratumoral Administration

To determine if the C225-G5-MTX bioconjugate could be used to specifically target EGFR in F98_{EGFR} glioma-bearing rats, [^{131}I]C225-G5-MTX was given by CED via the entry port of a plastic screw that had been embedded in the calvarium of rats bearing either F98_{WT} or F98_{EGFR} gliomas. After 24 hours, radioactivity in tumor and normal brain was measured by γ -scintillation counting. As shown in Fig. 6, the mean radioactivity was $62.7 \pm 14.7\%$ ID/g tumor in rats bearing F98_{EGFR} gliomas compared with $11.3 \pm 3.6\%$ ID/g tumor in rats bearing F98_{WT} gliomas, thereby demonstrating specific targeting of EGFR. The corresponding amounts in normal brain from the F98_{EGFR} tumor-bearing right (ipsilateral) and non-tumor-bearing left (contralateral) cerebral hemispheres were $5.8 \pm 3.4\%$ and $0.8 \pm 0.6\%$ ID/g tissue, respectively. Blood, liver, kidneys, spleen, and skin all had negligible levels of radioactivity ($<0.5\%$ ID/g tissue). The tumor/brain ratio for EGFR-positive gliomas was 10.8. There was 5.5-fold difference in retention of the bioconjugate in EGFR-positive versus EGFR-negative tumors at 24 hours after administration, thereby showing that clearance of the bioconjugate from rats bearing F98_{EGFR} was significantly slower.

Therapy Studies

Based on the promising results of the biodistribution study, a pilot therapy study was initiated 7 days following i.c. implantation of 10^5 F98_{EGFR} glioma cells. Animals received cetuximab, C225-G5-MTX, or free methotrexate by CED, which was well tolerated, and then weighed thrice weekly and their clinical status was monitored until the time of death or euthanization. The Kaplan-Meier survival

curves are shown in Fig. 7. Rats that received C225-G5-MTX cetuximab had mean survival time of 16 ± 3 , 17 ± 2 , and 19 ± 4 days compared with 15 ± 2 days for untreated controls. The corresponding median survival times were 15, 17, 19.5, and 15 days, respectively, and the ranges were between 12 and 25 days. As determined by Gehan's Wilcoxon rank sum test, the mean survival time of animals that received the bioconjugate was not significantly different from those of animals that received either methotrexate ($P = 0.056$) or cetuximab ($P = 0.42$).

Brain Histopathology

The brains of all rats were subjected to histopathologic examination following staining with H&E. Tumors from untreated animals were composed of fusiform tumor cells having variably whorled (storiform) pattern of growth (Fig. 8A). Large tumors showed central areas of necrosis. Tumors from animals that received the bioconjugate showed focal areas of necrosis with disaggregation of the nuclei, clumping of nuclear chromatin, and karyolysis or karyorrhexis (Fig. 8B). Tumors from animals that received methotrexate alone showed either no necrosis or small focal areas of necrosis (Fig. 8C). In contrast, animals that received cetuximab alone showed cellular morphologic changes consistent with apoptosis (34), with prominent condensation and clumping of nuclear chromatin without concomitant karyolysis or karyorrhexis (Fig. 8D). However, tumors from three other animals in this group of seven did not show either necrosis or focal necrotic areas. To better characterize the morphologic differences in tumor histopathology, immunostaining was carried out for Bcl-2, as a surrogate marker for apoptosis, and MIB-1 (Ki-67) to identify proliferating cells. The former was positive, confirming the presence of apoptotic cells that had been identified morphologically. Immunostaining with MIB-1 (Ki-67) did not reveal any differences between untreated control animals and those that had received either cetuximab or methotrexate.

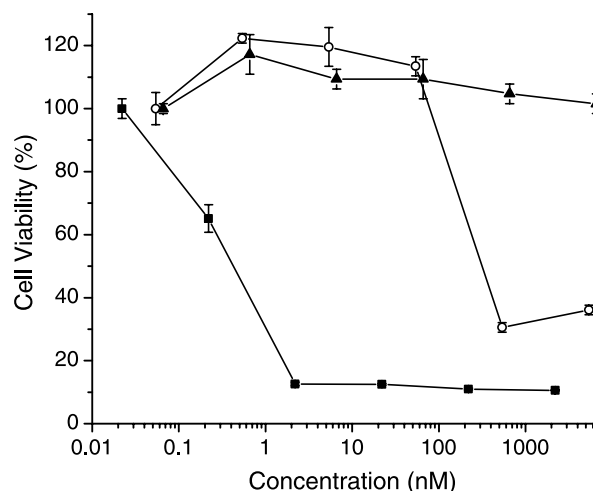


Figure 5. Cell viability as determined by the sulforhodamine B assay. F98_{EGFR} cells were incubated with methotrexate (■), C225-G5-MTX (○), or cetuximab (▲) for 72 h, after which sulforhodamine B was added. Absorbance was determined at 490 nm in a microplate reader.

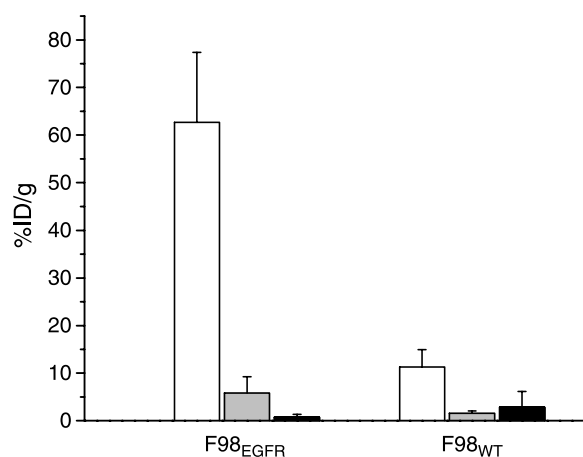


Figure 6. Biodistribution of [^{131}I]C225-G5-MTX following CED to rats bearing i.c. implants of F98_{EGFR} or F98_{WT} gliomas. Animals were euthanized 24 h after injection, the tumor (□) was dissected, and the radioactivity in tumor and right (right brain; ▣) and left (left brain; ■) cerebral hemispheres was quantified by γ -scintillation counting. Mean \pm SD.

Discussion

In the present study, we have described the construction and characterization of a bioconjugate that was designed to deliver methotrexate to tumor cells overexpressing either EGFR or EGFRvIII. Based on the molecular weight of the bioconjugate, an average of 12.6 molecules of methotrexate were linked to each fifth-generation PAMAM dendrimer molecule, which subsequently was conjugated to cetuximab. The bioconjugate showed a small reduction in EC₅₀ (0.8 log unit), but the cytotoxicity was 2.7 log units lower than that of the free methotrexate. As shown by *in vivo* biodistribution studies, the bioconjugate was selectively retained in rats bearing i.c. implants of the F98_{EGFR} glioma. However, no therapeutic gain was observed in tumor-bearing animals that received the bioconjugate by CED compared with those that received free methotrexate or cetuximab.

Coupling methotrexate to a fifth-generation PAMAM dendrimer was carried out with 1-ethyl-3(3-dimethylaminopropyl)carbodiimide hydrochloride and *N*-hydroxysuccinimide. The number of methotrexate molecules linked to the dendrimer (12.6) was found to be much lower than the number of reactive primary amine groups on the fifth-generation polyamidoamine dendrimer. There are two possible explanations for this. (a) The number of molecules of methotrexate attached to each dendrimer molecule was limited by its water solubility. (b) The 1-ethyl-3(3-dimethylaminopropyl)carbodiimide hydrochloride method used to conjugate methotrexate to the dendrimer may have activated both α - and γ -carboxyl groups, thereby linking one methotrexate molecule to two primary amine groups on the surface of the PAMAM dendrimer. This could also provide an explanation for the reduced *in vitro* cytotoxicity of the bioconjugate. It has been reported that free α -carboxyl groups are necessary for methotrexate to tightly bind to its target enzyme dihydrofolate reductase (35). Similar

phenomena also have been observed for methotrexate-branched polypeptide conjugates. Methotrexate conjugated to amphoteric polymers resulted in \sim 500-fold reduction of anti-791T cytotoxic activity, and conjugation with the polycationic carrier (LAK-MTX) reduced cytotoxicity 60 times compared with that of free methotrexate (36).

Methotrexate has been linked to a variety of carriers, such as gelatin (37), polyethylene glycol (38), transferrin (39), human (40), and rat serum albumin (41), polylysine (42, 43), carboxymethyl cellulose (44), and dextran (45), to improve its therapeutic index. Recently, polyamidoamine dendrimers have been used as a drug delivery platform and these have shown unique properties, such as a high degree of molecular uniformity, narrow molecular weight distributions, specific size and shape characteristics, and a highly functionalized terminal surface (46). In our own previous studies, methylisocyanato polyhedral borane anions were attached to the dendrimer by the reaction of isocyanate with amines on the dendrimer surface (25). A total of \sim 110 polyhedral borane anions were linked to a fifth generation PAMAM dendrimer. In addition, there have been attempts at site-specific targeting using dendrimers. It recently has been reported that acetylated dendrimer-methotrexate could be conjugated to folic acid for use as a targeting agent. The conjugate showed tumor selectivity, decreased toxicity, and increased antitumor activity (47).

The major limitation in using anti-EGFR mAbs clinically to treat patients with brain tumors has been that extraordinarily small quantities reached the tumor following systemic administration (48, 49). This has been attributed to a combination of their rapid clearance by the reticulo-endothelial system and the blood-brain barrier, which prevents the passage of hydrophilic agents with a molecular weight more than \sim 250 Da unless there is an active transport system (50). Direct i.c. delivery of a mAb

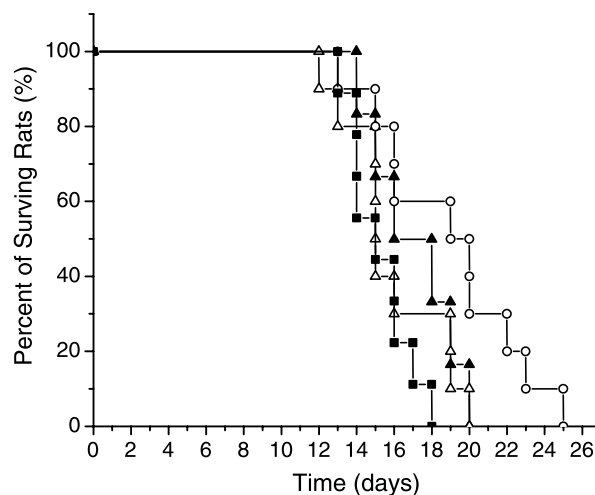


Figure 7. Kaplan-Meier survival curves for F98_{EGFR} glioma-bearing rats. Rats were untreated (■) or treated with cetuximab (C225; ▲), C225-G5-MTX (△), and free methotrexate (○) 1 wk after implantation of 10^5 F98_{EGFR} cells.

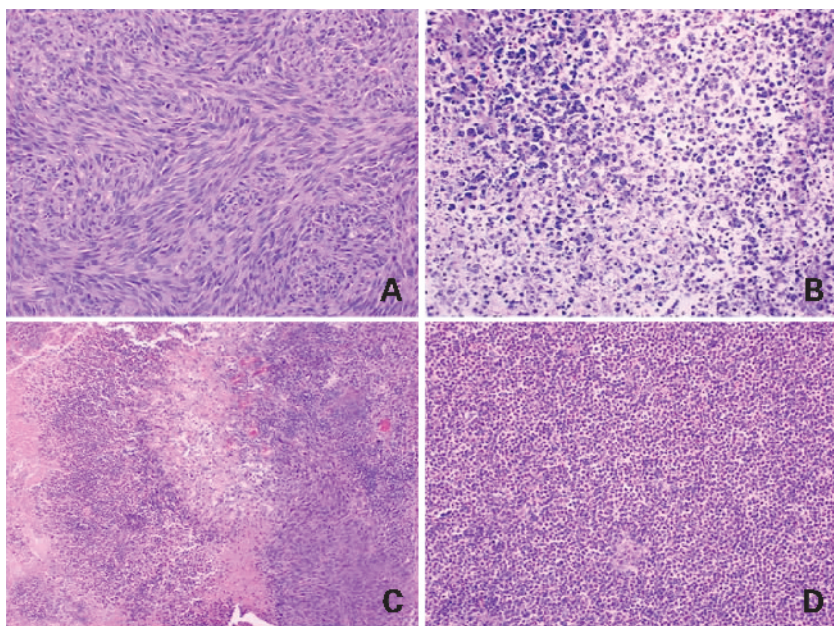


Figure 8. Histopathologic characteristic of F98^{EGFR} gliomas from untreated and treated Fischer rats bearing i.c. tumor implants. One week following tumor implantation, animals treated with the test agent were euthanized 1 to 2 d before their estimated date of death. Brains were removed, fixed, and then processed for histopathologic examination. The sections were stained with H&E. Magnification, $\times 200$. Untreated control animals (A), F98^{EGFR} glioma-bearing rats treated with C225-G5-MTX (B), methotrexate (C), and cetuximab (D).

by CED can bypass the blood-brain barrier, minimize the toxicity associated with systemic administration, and reduce by orders of magnitude the amount of the mAb or bioconjugate that would have to be given (30, 32). We previously have used CED to administer the mAb L8A4 to F98^{EGFR^{VIII}} and cetuximab to F98^{EGFR} glioma-bearing rats (51). The biodistribution of [¹³¹I]C225-G5-MTX, given by CED, resulted in $62.7 \pm 14.7\%$ ID/g tumor being retained in EGFR-positive gliomas versus $11.3 \pm 3.6\%$ ID/g tumor in F98^{WT} receptor-negative tumors (28). In contrast, normal brain from the tumor-bearing cerebral hemisphere had $5.8 \pm 3.4\%$ ID/g and the blood and extracranial tissues had $<0.5\%$ ID/g. These results confirm the superiority of direct i.c. administration by means of CED of brain tumor-targeting agents to maximize tumor drug concentrations and minimize their concentration in other organs.

The mechanisms of cytotoxicity and selectivity of methotrexate depend on the inhibition of its target, the folate-dependent enzyme dihydrofolate reductase, dTMP synthesis, and *de novo* purine synthesis. These inhibit DNA synthesis and subsequently lead to cell death. Due to the toxicity of methotrexate, considerable effort has been devoted to the design of more selective cytoreductive antifolates. However, none of these were better than methotrexate (52). Although in our study there was specific molecular targeting of C225-G5-MTX to EGFR-positive gliomas, disappointingly, the survival times were not significantly different between the experimental groups that received cetuximab, C225-G5-MTX, and free methotrexate. What might be the explanation for this? One possibility is that linkage of methotrexate to a macromolecular species, such as a PAMAM dendrimer, to a mAb altered its binding affinity with dihydrofolate reductase and subsequently lost its antifolate activity. Alternatively, the methotrexate linked to the dendrimer may not have

been released and therefore was not cytotoxic. To circumvent this problem, a cleavable linker could be used to attach methotrexate to the dendrimer (53), so that the bioconjugate would retain both tumor selectivity and antifolate activity. Nevertheless, even if the bioconjugate and free drug had equivalent therapeutic activity, it is possible that the bioconjugate might be superior due to its reduced toxicity for normal brain due to specific targeting of tumor cells.

In conclusion, we have constructed a specific tumor-targeting drug delivery system with an increased methotrexate payload. This principle could be applied to the delivery of either one or multiple drugs to enhance their therapeutic index or to imaging agents to improve their diagnostic potential (54). Our results, which are both positive and negative, show that specific molecular targeting is but one of several requirements that must be fulfilled if an antibody-drug bioconjugate will be therapeutically useful.

Acknowledgments

We thank Dr. Daniel Hicklin for a generous gift of cetuximab to carry out these studies, Michele Swindall and Nan Kleinholz for technical assistance, and Michelle Smith and Beth Kahl for secretarial assistance in the preparation of this article.

References

- Garnett MC. Targeted drug conjugates: principles and progress. *Adv Drug Deliv Rev* 2001;53:171–216.
- Hamblett KJ, Senter PD, Chace DF, et al. Effects of drug loading on the antitumor activity of a monoclonal antibody drug conjugate. *Clin Cancer Res* 2004;10:7063–70.
- Trail PA, King HD, Dubowchik GM. Monoclonal antibody drug immunoconjugates for targeted treatment of cancer. *Cancer Immunol Immunother* 2003;52:328–37.
- Mischel PS, Cloughesy TF. Targeted molecular therapy of GBM. *Brain Pathol* 2003;13:52–61.
- Payne G. Progress in immunoconjugate cancer therapeutics. *Cancer Cell* 2003;3:207–12.

6. Milenic DE. Monoclonal antibody-based therapy strategies: providing options for the cancer patient. *Curr Pharm Des* 2002;8:1749–64.
7. Graham CA, Cloughesy TF. Brain tumor treatment: chemotherapy and other new developments. *Semin Oncol Nurs* 2004;20:260–72.
8. Desjardins A, Rich JN, Quinn JA, et al. Chemotherapy and novel therapeutic approaches in malignant glioma. *Front Biosci* 2005;10:2645–68.
9. Mendelsohn J. The epidermal growth factor receptor as a target for cancer therapy. *Endocr Relat Cancer* 2001;8:3–9.
10. Bredel M, Pollack IF, Hamilton RL, James CD. Epidermal growth factor receptor expression and gene amplification in high-grade non-brainstem gliomas of childhood. *Clin Cancer Res* 1999;5:1786–92.
11. Lammering G, Hewit TH, Holmes M, et al. Inhibition of the type III epidermal growth factor receptor variant mutant receptor by dominant-negative EGFR-CD533 enhances malignant glioma cell radiosensitivity. *Clin Cancer Res* 2004;10:6732–43.
12. Herbst RS. Review of epidermal growth factor receptor biology. *Int J Radiat Oncol Biol Phys* 2004;59:21–6.
13. Kuan CT, Wikstrand CJ, Bigner DD. EGFRvIII as a promising target for antibody-based brain tumor therapy. *Brain Tumor Pathol* 2000;17:71–8.
14. Pedersen MW, Meltorn M, Damstrup L, Poulsen HS. The type III epidermal growth factor receptor mutation. Biological significance and potential target for anti-cancer therapy. *Ann Oncol* 2001;12:745–60.
15. Lorimer IA. Mutant epidermal growth factor receptors as targets for cancer therapy. *Curr Cancer Drug Targets* 2002;2:91–102.
16. Janmaat ML, Giaccone G. The epidermal growth factor receptor pathway and its inhibition as anticancer therapy. *Drugs Today (Barc)* 2003;39 Suppl C:61–80.
17. Normanno N, Maiello MR, Mancino M, De Luca A. Small molecule epidermal growth factor receptor tyrosine kinase inhibitors: an overview. *J Chemother* 2004;16 Suppl 4:36–40.
18. Goldberg RM. Cetuximab. *Nat Rev Drug Discov* 2005;Suppl:S10–1.
19. Harding J, Burtneß B. Cetuximab: an epidermal growth factor receptor chimeric human-murine monoclonal antibody. *Drugs Today (Barc)* 2005;41:107–27.
20. Khamly K, Jefford M, Michael M, Zalberg J. Beyond 5-fluorouracil: new horizons in systemic therapy for advanced colorectal cancer. *Expert Opin Investig Drugs* 2005;14:607–28.
21. Venook A. Critical evaluation of current treatments in metastatic colorectal cancer. *Oncologist* 2005;10:250–61.
22. Safavy A, Bonner JA, Waksal HW, et al. Synthesis and biological evaluation of paclitaxel-C225 conjugate as a model for targeted drug delivery. *Bioconjug Chem* 2003;14:302–10.
23. Mamot C, Nguyen JB, Pourdehnad M, et al. Extensive distribution of liposomes in rodent brains and brain tumors following convection-enhanced delivery. *J Neuro Oncol* 2004;68:1–9.
24. Allegra CJ, Grem JL, Antimetabolites. Section 6. In: DeVita VT, Jr., Hellman S, Rosenberg SA, editors. *Cancer: principles and practice of oncology*. Philadelphia: Lippincott-Raven; 1997. pp. 432–6.
25. Wu G, Barth RF, Yang W, et al. Site-specific conjugation of boron-containing dendrimers to anti-EGF receptor monoclonal antibody cetuximab (IMC-C225) and its evaluation as a potential delivery agent for neutron capture therapy. *Bioconjug Chem* 2004;15:185–94.
26. Barth RF. Rat brain tumor models in experimental neuro-oncology: the 9L, C6, T9, F98, RG2 (D74), RT-2, and CNS-1 gliomas. *J Neuro Oncol* 1998;36:91–102.
27. Barth RF, Yang W, Rotaru JH, et al. Boron neutron capture therapy of brain tumors: enhanced survival and cure following blood-brain barrier disruption and intracarotid injection of sodium borocaptate and boronophenylalanine. *Int J Radiat Oncol Biol Phys* 2000;47:209–18.
28. Barth RF, Wu G, Yang W, et al. Neutron capture therapy of epidermal growth factor (+) gliomas using boronated cetuximab (IMC-C225) as a delivery agent. *Appl Radiat Isot* 2004;61:899–903.
29. Yang W, Barth RF, Wu G, et al. Boronated epidermal growth factor as a delivery agent for neutron capture therapy of EGF receptor positive gliomas. *Appl Radiat Isot* 2004;61:981–5.
30. Barth RF, Yang W, Adams DM, et al. Molecular targeting of the epidermal growth factor receptor for neutron capture therapy of gliomas. *Cancer Res* 2002;62:3159–66.
31. Pauwels B, Korst AE, de Pooter CM, et al. Comparison of the sulforhodamine B assay and the clonogenic assay for *in vitro* chemoradiation studies. *Cancer Chemother Pharmacol* 2003;51:221–6.
32. Yang W, Barth RF, Adams DM, et al. Convection-enhanced delivery of boronated epidermal growth factor for molecular targeting of EGF receptor-positive gliomas. *Cancer Res* 2002;62:6552–8.
33. Klein JP, Moeschberger ML. Survival analysis: techniques for censored and truncated data. 2nd ed. New York: Springer; 2003. p. xv, 536.
34. Jordan LB, Harrison DJ. Apoptosis and cell senescence in molecular biology in cellular pathology. In: Crocker J, Murray PG, editors. Hoboken (NJ): John Wiley & Sons; 2003. p. 153–92.
35. Rosowsky A, Forsch RA, Moran RG, Kohler W, Freisheim JH. Methotrexate analogues. 32. Chain extension, α -carboxyl deletion, and γ -carboxyl replacement by sulfonate and phosphonate: effect on enzyme binding and cell-growth inhibition. *J Med Chem* 1988;31:1326–31.
36. Hudecz F, Clegg JA, Kajtar J, et al. Influence of carrier on biodistribution and *in vitro* cytotoxicity of methotrexate-branched polypeptide conjugates. *Bioconjug Chem* 1993;4:25–33.
37. Kosasih A, Bowman BJ, Wigent RJ, Ofner CM, III. Characterization and *in vitro* release of methotrexate from gelatin/methotrexate conjugates formed using different preparation variables. *Int J Pharm* 2000;204:81–9.
38. Riebeseel K, Biedermann E, Loser R, et al. Polyethylene glycol conjugates of methotrexate varying in their molecular weight from MW 750 to MW 40000: synthesis, characterization, and structure-activity relationships *in vitro* and *in vivo*. *Bioconjug Chem* 2002;13:773–85.
39. Singh M. Transferrin As A targeting ligand for liposomes and anticancer drugs. *Curr Pharm Des* 1999;5:443–51.
40. Burger AM, Hartung G, Stehle G, Sinn H, Fiebig HH. Pre-clinical evaluation of a methotrexate-albumin conjugate (MTX-HSA) in human tumor xenografts *in vivo*. *Int J Cancer* 2001;92:718–24.
41. Stehle G, Wunder A, Schrenk HH, et al. Methotrexate-albumin conjugate causes tumor growth delay in Dunning R3327 HI prostate cancer-bearing rats. *Anticancer Drugs* 1999;10:405–11.
42. Ryser HJ, Mandel R, Hacobian A, Shen WC. Methotrexate-poly(l-lysine) as a selective agent for mutants of Chinese hamster ovary cells defective in endocytosis. *J Cell Physiol* 1988;135:277–84.
43. Ryser HJ, Shen WC. Conjugation of methotrexate to poly (l-lysine) as a potential way to overcome drug resistance. *Cancer* 1980;45:1207–11.
44. Fung WP, Przybylski M, Ringsdorf H, Zaharko DS. *In vitro* inhibitory effects of polymer-linked methotrexate derivatives on tetrahydrofolate dehydrogenase and murine L5178Y cells. *J Natl Cancer Inst* 1979;62:1261–4.
45. Dang W, Colvin OM, Brem H, Saltzman WM. Covalent coupling of methotrexate to dextran enhances the penetration of cytotoxicity into a tissue-like matrix. *Cancer Res* 1994;54:1729–35.
46. Gillies ER, Frechet JM. Dendrimers and dendritic polymers in drug delivery. *Drug Discov Today* 2005;10:35–43.
47. Kukowska-Latallo JF, Candido KA, Cao Z, et al. Nanoparticle targeting of anticancer drug improves therapeutic response in animal model of human epithelial cancer. *Cancer Res* 2005;65:5317–24.
48. Brady LW, Myamoto C, Woo DV, et al. Malignant astroglomas treated with iodine-125 labeled monoclonal antibody 425 against epidermal growth factor receptor: a phase II trial. *Int J Radiat Oncol Biol Phys* 1992;22:225–30.
49. Faillot T, Magdelenat H, Mady E, et al. A phase I study of an anti-epidermal growth factor receptor monoclonal antibody for the treatment of gliomas. *Neurosurgery* 1996;39:478–83.
50. Loscher W, Potschka H. Role of drug efflux transporters in the brain for drug disposition and treatment of brain diseases. *Prog Neurobiol* 2005;76:22–76.
51. Yang W, Barth RF, Wu G, et al. Development of a syngeneic rat brain tumor model expressing EGFRvIII and its use for molecular targeting studies with monoclonal antibody L8A4. *Clin Cancer Res* 2005;11:341–50.
52. McGuire JJ. Anticancer antifolates: current status and future directions. *Curr Pharm Des* 2003;9:2593–613.
53. Saito G, Swanson JA, Lee KD. Drug delivery strategy utilizing conjugation via reversible disulfide linkages: role and site of cellular reducing activities. *Adv Drug Deliv Rev* 2003;55:199–215.
54. Kobayashi H, Brechbiel MW. Dendrimer-based nanosized MRI contrast agents. *Curr Pharm Biotechnol* 2004;5:539–49.